Eclipse-Free Three-Body Periodic Orbits in Cislunar Space

Samuel Wishnek
Ball Aerospace
Joshua Wysack
Ball Aerospace

Jeremy Correa
Ball Aerospace

ABSTRACT

Long eclipse times in cislunar space can increase power storage and thermal management requirements on a spacecraft. Avoiding eclipses can help mitigate these issues. Several approaches are taken to study cislunar periodic orbits in terms of their eclipse times. L1 halo, L2 halo, vertical, axial, and Lyapunov orbits are all investigated. Applying a grid search, genetic algorithm, and analytical analysis of resonant orbits, we find trajectories that remain eclipse-free for a two year example mission as well as orbits that remain long-term eclipse-free while in resonance with the Moon's synodic orbital period. Tools to find near trajectories under higher-fidelity dynamics are then discussed as well as the application of these orbits to space domain awareness.

1. INTRODUCTION

With the increase of planned activity in the cislunar and lunar space environments, there is a need for mature mission designs that can accommodate the practical challenges with these environments. The Earth-Moon Lagrange point L1 is an advantageous location for many mission areas, including space domain awareness (SDA), space traffic management (STM), communication, and position, navigation, and timing (PNT). Orbits near L1 provide an excellent vantage point to view objects on Earth-Moon return or depart missions as well as in lunar orbit, which is particularly favorable for SDA and STM [1].

Many orbits in cislunar space have long eclipse durations due to both the Earth and the Moon. Earth eclipses can last up to 6 hours, while Moon eclipses can last up to 15 hours. For thermal and power reasons, these eclipse durations are not acceptable for many missions. Long duration eclipses such as these can require larger batteries to maintain power. In this paper, we explore optimal trajectory design to mitigate these lengthy shadow times. Strategies include phasing of the orbit to remain out of the penumbra of these bodies and choosing orbit geometry to reduce eclipses.

Orbit selection plays an important role as families of orbits experience different eclipse durations as a result of satellite-Earth-Moon-Sun geometry as well as orbit size and energy. Orbits in the L1 regime do not remain stable under high-fidelity propagation, so a robust station-keeping strategy is required. More fuel-conscious strategies to station-keeping also allow the satellite to drift away from the ideal halo orbit and this needs to be accounted for in tracking potential eclipse events. This paper presents realistic station-keeping and eclipse mitigation strategies from both an idealized and realistic viewpoint.

Much of the analysis is performed under circular restricted three body problem (CR3BP) dynamics. Under this simplified model, a large number of scenarios can be analyzed relatively quickly. However, as this model substantially deviates from truth, follow-up analysis is performed with a more accurate model using planetary ephemeris from JPL's SPICE toolkit [2]. This paper includes discussion on finding CR3BP orbits and then translating them to close orbits under higher-fidelity dynamics.

In addition, the relationship between long-term eclipse-free orbits and orbits in resonance with the Moon's synodic period is explored. An inequality is presented that must be satisfied for a resonant orbit to remain long-term eclipse-free. This work improves upon the state of the art by accounting for the relationship between this resonance and the initial phase and thoroughly exploring the orbits that satisfy the required conditions [3].

Here we present an exploration of eclipse-free cislunar orbits. This includes a genetic algorithm approach to finding these orbits, an analytical method for checking if orbits are long-term eclipse-free, and an approach for verifying this under higher-fidelity dynamics. This is presented along with an investigation into a specific case of a two year eclipse-free L1 halo orbit as an illustrative example.

2. THEORY

2.1 Generating Circular Restricted Solutions

The circular restricted case is well-studied and cataloged. Publically accessible tools such as JPL's Three Body Periodic Orbits website allow for easy generation of solutions under these simplified dynamics [4]. Furthermore, with a close approximate to an initial state, a precise solution for any three-body periodic orbit can be found with the single-shooting method [5]. The single-shooting method is an iterative method to find initial conditions that will propagate into a closed periodic orbit. It works by taking a trial solution, propagating it forward until it either crosses back over the plane that it stated in or the time reaches some set upper limit. The error between the start position and final position is treated as a cost and the initial conditions are updated to minimize it. A minimum norm update as shown in equation (1) can be used to perform the initial condition update. In this equation x is the trial state, $f(x)$ is the vector of constraints, and $\nabla f(x)$ is the gradient of $f(x)$. So long as the initial guess is sufficiently close to the solution, the trial state will adjust down the direction of the gradient and converge onto a solution that minimizes the error between the propagated final state and the goal. Symmetries in certain periodic three-body orbits allow for further simplifications. For example, L1 halo orbits will orthogonally intersect the circular restricted X-Z plane. So the velocity will be entirely in the Y direction at that point. Under these assumptions, equation (1) simplifies to equation (2). There $\Phi a,b$ is the row a and column b element of the state transition matrix for the propagation of the orbit for one period and all the other terms are the state elements expressed in the CR3BP frame.

$$x_{j+1} = x_j - \nabla f^T(x)\left(\nabla f(x)\nabla f^T(x)\right) f(x) \tag{1}$$

$$\begin{bmatrix} z_{j+1} \\ \dot{y}_{j+1} \end{bmatrix} = \begin{bmatrix} z_j \\ \dot{y}_j \end{bmatrix} - \left(\begin{bmatrix} \Phi_{4,3} & \Phi_{4,5} \\ \Phi_{6,7} & \Phi_{6,5} \end{bmatrix} - \frac{1}{\dot{y}_j} \begin{bmatrix} \ddot{x}_j \\ \ddot{z}_j \end{bmatrix} \begin{bmatrix} \Phi_{2,3} & \Phi_{2,5} \end{bmatrix} \right)^{-1} \begin{bmatrix} \dot{x}_j \\ \dot{z}_j \end{bmatrix} \tag{2}$$

2.2 Generating higher-fidelity Solutions

While circular restricted three-body dynamics are a useful tool for approximating orbits, they substantially differ from the real dynamics a satellite in that environment would face. The eccentricity of the Moon's orbit shifts the distance between the Earth and Moon over each period. The Moon and Earth's geopotential model does not act as a perfect point source. Solar radiation pressure adds an acceleration away from the direction of the Sun [6]. These forces are not perfectly periodic with either the motion of the satellite or the Moon itself. Accordingly, solutions are bound to the time of the physical scenario they were solved under. A solution at one time will not accurately model a feasible solution at most others.

The single-shooting method works well under the simplified circular restricted three body problem dynamics, but it is far less reliable when the dynamics diverge away from that model [7]. In order to converge to a solution, it must remain close enough to that solution such that small corrections to its state will keep it in that neighborhood. For higher-fidelity dynamics, the assumptions that allow the single-shooting method search space to be simplified to search over less dimensions are no longer valid. For example, a halo orbit may no longer perfectly intersect the Earth-Moon orbital plane orthogonally. To approach the problem without these assumptions, the multiple-shooting method can be applied [8]. Multiple shooting breaks the problem into smaller parts. Rather than only considering the initial condition propagated to some final time, multiple shooting considers several points along the trajectory. Each of these points are propagated only to the time of the next point. The solution space is also much larger. For finding halo orbits, the position states, velocity states, and time of each point can be allowed to move to find the solution. The shorter propagations for each step help keep erroneous solutions from diverging from the intended physical scenario. This helps keep periodic three-body orbits in the intended neighborhood of solutions. A minimum norm or optimization-based approach can then be applied to iterativelly converge onto a set of nodes that model a valid orbit under the more complex dynamics.

Since the dynamics under this higher-fidelity model depend on the planetary ephemeris, the solution cannot be appended to itself in order to extend its duration. Rather, the nodes must span multiple orbits in order to find a solution that allows for a passive near-periodic orbit over multiple revolutions. The solutions are also bound to the times they were solved at. This means that a new solution will need to be found if the start time of the required orbit changes.

2.3 Station-Keeping

The multiple shooting method can be adapted to provide a long-term station-keeping solution when modeling orbits. A single implementation of the multiple shooting algorithm can find a passive trajectory for some finite number of periods. However, due to both practical computational limits as well as real limits on the feasible duration of a completely passive trajectory, the solution cannot extend forever [9]. Rather, a station-keeping approach can be found by implementing the multiple-shooting method for an multiple-orbit solution, then taking that solution at a future node, fixing the start position and time to match the original solution, and extending out the solution space an equal number of nodes to those skipped. This can be run through multiple-shooting again. This time the solution will start very close to the previous solution but it will be unconcerned with earlier states while accounting for later states. The fixed initial position and time will allow only the initial velocity to adjust, so the difference between the original and updated trajectory can provide a delta-v for a planned maneuver at that point. By overlapping the runs, the second solution should remain closer to the original solution to hopefully provide a more feasible station-keeping cost [8].

2.4 Detection of Eclipse Events

With an ephemeris history generated with the multiple shooting method, detecting eclipse events can be performed by checking the relative positions of the satellite, Sun, and the Earth or Moon as occulting bodies at each point. One option is to generate the trajectory from the solution nodes and use an eclipse event finding tool such as SPICE's gfoclt_c to catch eclipse events [2]. An alternative solution is to generate the satellite's ephemeris for the full state history and check the positions of the bodies. Eclipses can be manually detected this way by checking at each point if the sum of the angular radius of the Sun and occulting body is less than the angular distance between the two bodies from the point of view of the satellite. If the sum is less than the distance, the Sun is at least partially eclipsed. This allows for the use of separate tools for propagating orbits and checking eclipses as small differences in orbit propagators may yield diverging trajectories. The inequality that must be satisfied to show that the object is not in eclipse is given in equation (3). There θ is the angle between the observed positions of the Sun and the occulting body, $R_\oplus$ and $R_\odot$ are the radii of the occulting body and Sun respectively, and $d_\oplus$ and $d_\odot$ are the distances from the object to the occulting body and the Sun respectively.

$$\theta \geq \arctan\left(\frac{R_\odot}{d_\odot}\right) + \arctan\left(\frac{R_\oplus}{d_\oplus}\right) \tag{3}$$

2.5 Resonance and Eclipses

For the purpose of avoiding eclipses, the Moon's mean synodic period of 29.53059 days is an important parameter for finding orbits with few eclipse events [10]. The 5.15 degree angle between the lunar orbital plane and the ecliptic means that the apparent position of the Sun will shift over at each conjunction of the Earth and Sun from the spacecraft's point of view. For eclipses by the Earth, the minimum height above or below the Moon's orbital plane that a space object must be at conjunction in order to avoid an eclipse no matter the relative position of the Sun is given by equation (4). i_M is the inclination of the Moon's orbit. x, y, and z are the coordinates of the coordinates of the satellite with respect to the Earth and the z axis perpendicular to the Moon's orbital plane. $R_\oplus$ is the radius of the Earth and $R_\odot$ is the radius of the Sun.

$$z = \sqrt{x^2+y^2}\tan\left(i_M + \arctan\left(\frac{R_\oplus}{\sqrt{x^2+y^2}}\right) + \arctan\left(\frac{R_\odot}{1AU}\right)\right) \tag{4}$$

Applying equation (4) to a periodic orbit in resonance with the Moon's synodic period allows for the detection of permanently eclipse-free periodic orbits. By phasing the orbit such that the object is maximally out of plane at the conjunction of the Earth and Sun, as long as the out-of-plane component of the object's position is greater than the result of equation (4), the object will not pass through the Earth's penumbra at any point.

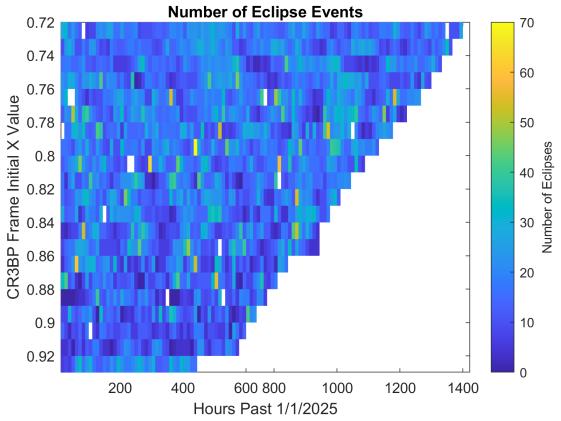

Fig. 1: Sampled northern L1 halo eclipse count.

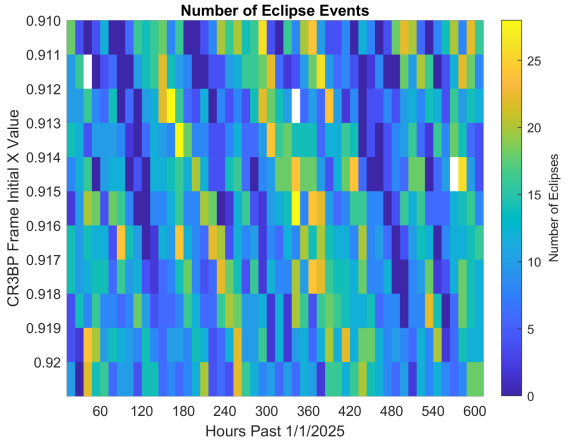

Fig. 2: Sampled eclipse counts near low eclipse regions.

2.6 Space Domain Awareness Application

3. RESULTS

3.1 Eclipses over Two Year Mission

First, an empirical approach was taken to study a particular scenario. The goal was to find reduced or eclipse-free orbits in the L1 environment for a two-year mission starting in January 2025. Two approaches were taking for this problem. One was a brute-force study of the feasible periodic orbits by applying a grid search to the problem. The other approach used a genetic algorithm to search for minimal eclipse trajectories fitting this problem.

3.1.1 Grid Search

The grid search approach was used to study the full domain of the problem. Two independent variables were discretized for this scenario. The initial CR3BP X position of the satellite and the phase of the satellite's state within the periodic orbit. For a northern L1 halo orbit, the single-shooting method only requires a choice of the x-position and an initial guess for the full state to find a periodic solution. This is because the initial state is chosen such that the CR3BP Y position is zero and the CR3BP X and Z velocities are zero. The single-shooting method iterates over the CR3BP Z position and CR3BP Y velocity. The CR3BP X position is then the unique element that determines where along the manifold of solutions the orbit will lie [5]. For each solution found with the single-shooting method, the phase is sampled up to the period. For each case, the trajectory under CR3BP dynamics is found, and recorded as an ephemeris history spanning the two-year period. This is then ingested into a script that interfaces with Orekit to detect any eclipse events from either the Moon or Earth over the duration of the ephemeris [11].

Figure 1 shows the number of eclipse events at each sampled point for northern L1 halo orbits, while figure 2 shows a zoomed in version of a subset of the data in order to show more detail in a region with low eclipses. The phase was indirectly manipulated by shifting the start time of the trajectory and extending its duration to match the two-year requirement. Several eclipse-free trajectories from this study were discovered with additional analysis was performed on these cases. Nine of the cases in the original full-scale search shown in figure 1 were found to be eclipse free. The finer search shown in figure 2 found clusters of eclipse-free orbits around solutions.

The eclipse-free results from this study were investigated further. Figure 3 shows the displacement along the CR3BP x-axis of the initial state to the L1 point against the period of the orbit in the CR3BP frame represented as a fraction of the Moon's sidereal period. The figure shows that the eclipse free cases are distributed fairly evenly across the space and the period generally gets longer as these orbits move closer to the Earth. Figure 4 shows the stability index of the orbits. Stability index closer to one represent more stable orbits while a larger stability index is less likely to remain near the intended trajectory under a small perturbation. Again, eclipse-free results are fairly evenly distributed across

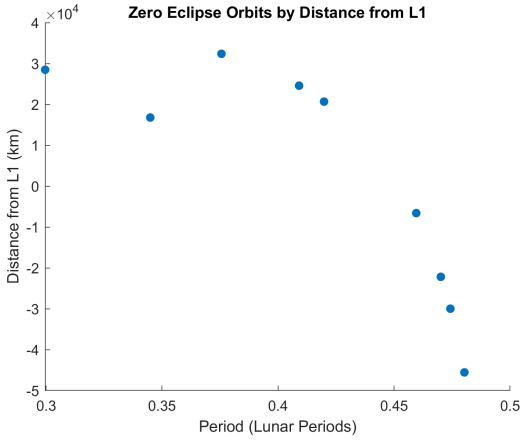

Fig. 3: Initial state displacement from L1 for sampled zero-eclipse orbits.

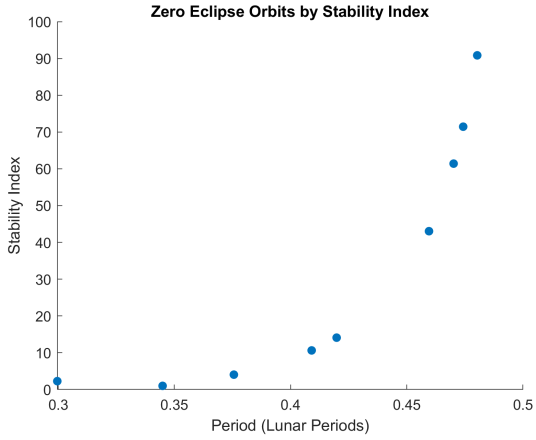

Fig. 4: Stability versus period for sampled zero-eclipse orbits.

the space and stability improves for shorter periods. The results for this grid-search approach show that for this type of mission, there are a wide variety of options for generating eclipse-free trajectories for the full two-year orbit period.

3.1.2 Genetic Algorithm Search

To better study the distribution of eclipse-free orbits. A genetic algorithm was applied to search the space of periodic three-body orbits. This is a more efficient approach than the grid search as it can avoid spending too much time in state space regions with frequent long eclipses. The genetic algorithm optimized over the same parameters as the grid search, initial phasing and the distance along the CR3BP X axis. This was finitely sampled by taking all provided cases from the JPL catalog for the given orbit type [4]. This was applied to northern and southern L1 halo orbits as well as L1 axial, Lyapunov, and vertical orbits. The results of this approach for the northern L1 halo orbits are shown in figures 5 and 6. Regions of the results with no eclipses are labeled and show up periodically in the results. The periodicity comes from the genetic algorithm's phase search spanning longer than a single CR3BP period, so results will be identical for identical phasings. The axial and vertical cases had a similar structure with regions of eclipse free orbits. However, the Lyapunov case had no eclipse-free results. This is likely due to the Lyapunov orbit being confined to the Earth-Moon orbital plane, so every crossing of the X-axis could potentially include an eclipse depending on the relative position of the Sun. The other orbits have enough motion out-of-plane to sometimes cross the X-axis far enough away from the Earth-Moon plane to avoid any possibility of eclipse.

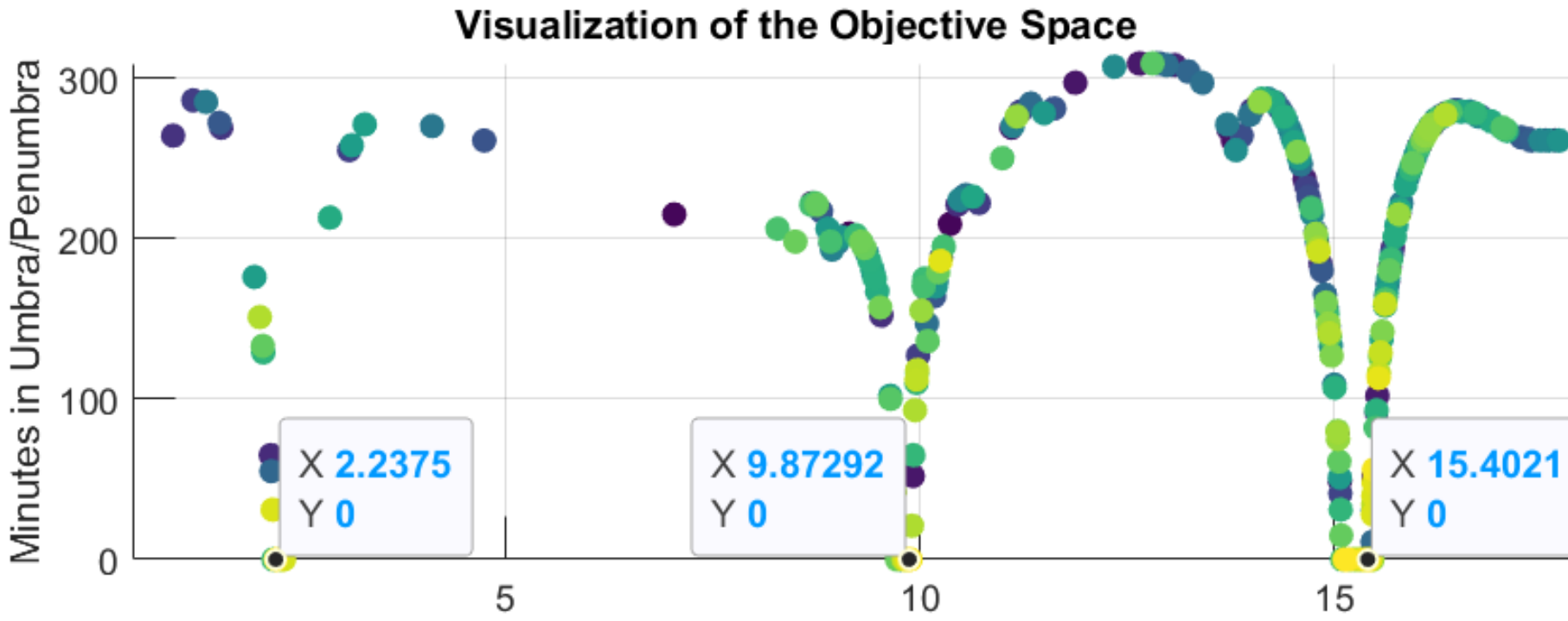

Fig. 5: Genetic algorithm results for minimizing eclipse time over a two-year northern L1 halo trajectory for early phasings.

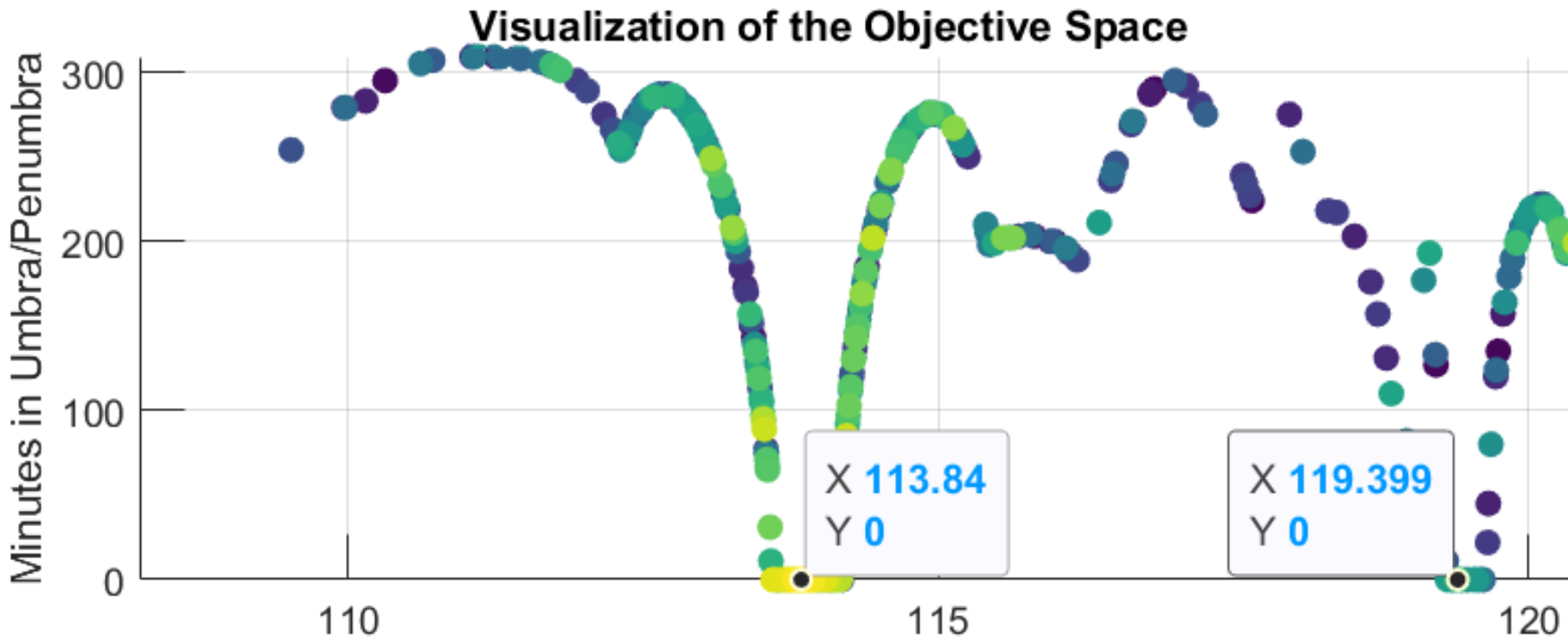

Fig. 6: Genetic algorithm results for minimizing eclipse time over a two-year northern L1 halo trajectory for late phasings.

3.1.3 higher-fidelity Trajectory

While results under CR3BP dynamics can approximate real solutions, there are significant differences between the real dynamics a space object will be under and these idealized approximations. In order to better estimate the true trajectories and eclipse histories for space objects, it is necessary to improve beyond the CR3BP model. The multiple shooting method described earlier is a useful tool for taking a CR3BP trajectory and finding a similar trajectory that follows a higher-fidelity model. Figure 7 shows the application of the multiple shooting method to a CR3BP trajectory for ten periods. Under these higher-fidelity dynamics, passive trajectories that approximate the idealized halo orbit do not close on themselves. The non-circular path of the Moon and the influence of other forces breaks the symmetry required to create the simple closed orbits found in the CR3BP dynamics. The application of the multiple shooting method is computationally intensive. Adjusting the genetic algorithm approach to use higher-fidelity dynamics would be much more computationally intensive. Rather, the approach taken was to find eclipse-free trajectories using the CR3BP dynamics. Choose the solution with the widest possible error bounds to remain eclipse-free, and use that trajectory to seed the multiple-shooting method. The resulting trajectory was then checked for eclipses.

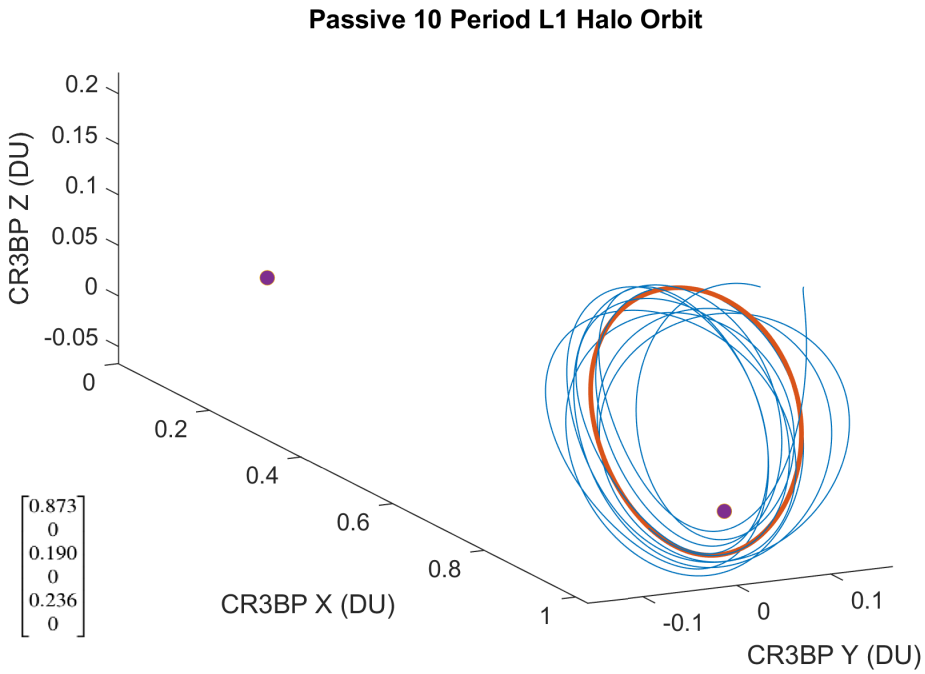

Fig. 7: CR3BP L1 halo orbit with 10 orbit solution found using multiple-shooting.

The L1 halo orbit in the middle of the first set of eclipse-free orbits in figure 6 was selected as the reference trajectory. The station-keeping approach described in section 2.3 was applied to this trajectory for eight months under higher-fidelity dynamics. The ephemeris of this trajectory was then assessed using the SPICE library to check for any eclipses. No eclipses were found for the duration.

3.2 Reduced Eclipse Phasing and Resonance

For northern L1 Halo orbits, the most easily achievable resonance with the Moon's synodic period is a three to one resonance. That would put the period of the orbit in the rotating frame at 9.844 days. The list of repeating orbits provided by the JPL's three-body periodic orbits website provides a close approximate halo orbit with period 9.846 days [4]. This solution was taken as initial guess and fed into an implementation of the single-shooting method wrapped inside a binary search to find a more precise match to the required period in CR3BP dynamics. The result was an orbit with period 9.844 days. This matched the goal period to less than one second error which is itself well below the magnitude of the regular fluctuations in the synodic period [10]. The resulting position and velocity initial

state in the rotating, Earth-Moon distance normalized frame is given below. The minimum height above the Moon's orbital plane to avoid eclipses as calculated by equation (4) is 0.0993 in the same frame. The calculated state nearly doubles that, so a satellite in this state with the maximal out of plane position phased to coincide with the syzygy of the Earth, Moon, and Sun would never enter eclipse under CR3BP dynamics.

By symmetry, there exists a southern halo orbit that matches this solution but is below the Earth-Moon plane at the required point. This orbit will also be eclipse-free. Lyapunov orbits are confined to the Earth-Moon plane and cannot be eclipse-free in this way [12]. Axial and vertical orbits have a minimum period too large to enable any resonance with the Moon's synodic period and therefore cannot be proven eclipse-free in this way [4]. The method can be applied for L2 orbits as well. A similar set of solutions can be found for L2 halo orbits. The results in 3:1 through 9:1 resonances are eclipse-free when appropriately phased. The 2:1 resonance does not rise high enough over the orbital plane to avoid eclipses this way. A summary of these results is shown in figure 8.

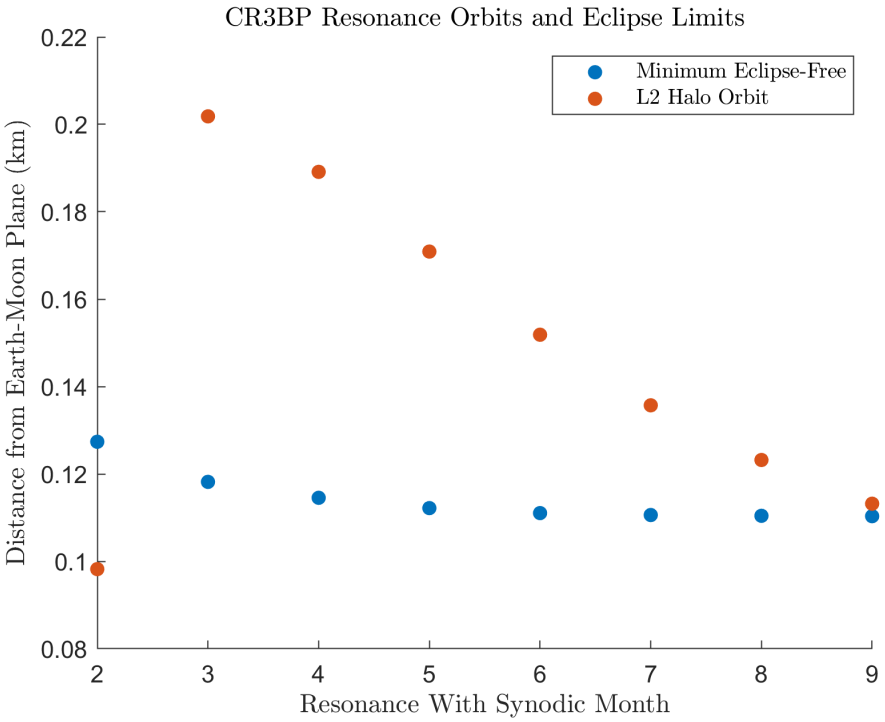

Fig. 8: L2 halo orbit comparison of maximum out-of-plane distance and required distance to avoid eclipses.

Since these results are based on CR3BP dynamics, the trajectory of a real object will not follow this precise path. The difference between the minimum required out-of-plane distance and the CR3BP trajectory shows the allowable error for the true trajectory to remain eclipse free.

3.3 Environment Visibility

These orbit families have different capabilities as platforms for space-based SDA optical sensors. In order to determine the observability of the environment from a satellite in one of these orbits, a model was generated treating targets as one meter diameter Lambertian spheres with twenty percent reflectivity. The analysis considers solar phase angle and relative visual magnitude to determine if a region is observable. Target regions include Earth-centered space from the geostationary orbital radius out to 3.4 times the radius of geostationary orbit and a lobe of space leading out to the Moon considered the cislunar corridor. This extends to ten thousand kilometers past L2 along the vector pointing from the Earth to the Moon.

Results for families investigated in this research, L1 halo, L2 halo, vertical, axial, and Lyapunov orbits are show in figure 10. There we see that while we did not find eclipse-free Lyapunov orbits, it has the best observability of the tested volume. On the other hand, while L2 halo orbit had several options for resonant eclipse-free orbits, they had the

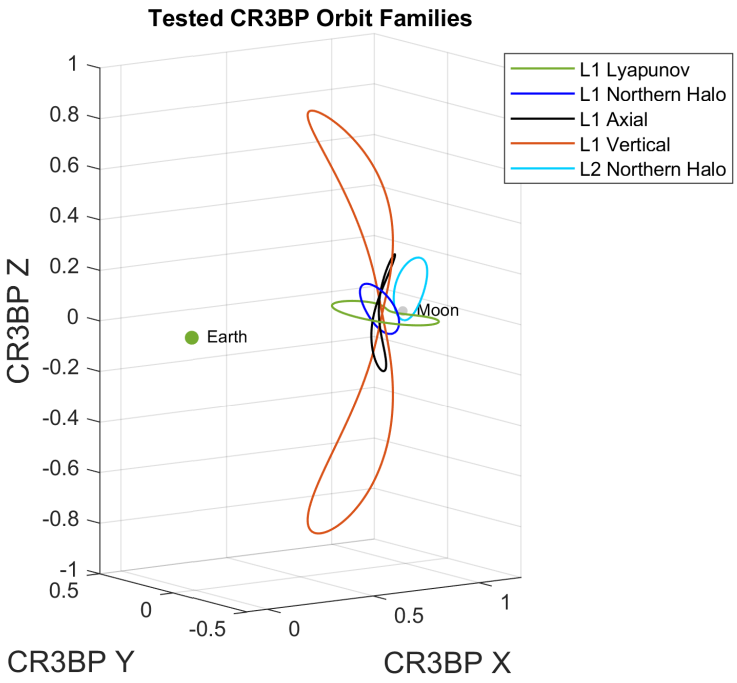

Fig. 9: Example CR3BP orbits for tested families.

lowest ability to observe the volume. This is largely due to the large distance between an object in an L2 halo orbit and a trial target which limits the relative magnitude of the target.

4. CONCLUSION

In this work, several different families if cislunar orbits were investigated to find orbits that reduced or completely avoided eclipses. Two forms of optimization were applied to minimize eclipse time. The first being the grid search, used to find a set of solutions over the space of orbit phasings and the initial state CR3BP X axis value. This showed a wide distribution eclipse-free trajectories for two-year missions across both axes. A follow-up analysis with a genetic algorithm confirmed this and also showed that eclipse-free orbits existed for L1 axial and vertical orbits. Orbits in resonance with the Moon's synodic period were then explored as potential cases for long-term eclipse-free periodic orbits. These were confirmed for the L1 halo 3:1 resonance orbit and the L2 halo 3:1 through 9:1 resonance orbits. The multiple-shooting method was then used to find a close estimate to the CR3BP trajectory in higher-fidelity dynamics and verify that some of the cases were eclipse free.

Follow-up research to this topic could include a more thorough application of the extension to higher-fidelity dynamics to verify each case is eclipse free. Due to computational constraints, only the illustrative examples were verified in this way for this work. Lunar orbits are another candidate for similar missions in this region, so extending this research to include true lunar orbits could provide additional feasible cases for eclipse mitigation with similar applicability to space domain awareness.

REFERENCES

[1] MJ Holzinger, CC Chow, and P Garretson. A primer on cislunar space. 2021.

[2] Charles H Acton Jr. Ancillary data services of nasa's navigation and ancillary information facility. *Planetary and Space Science*, 44(1):65–70, 1996.

[3] P Pergola and EM Alessi. Libration point orbit characterization in the earth–moon system. *Monthly Notices of the Royal Astronomical Society*, 426(2):1212–1222, 2012.

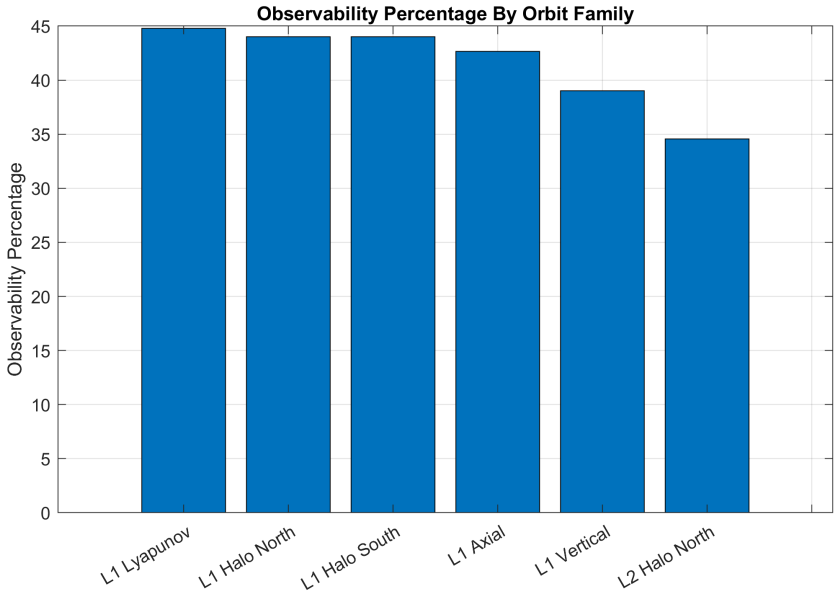

Fig. 10: L2 halo orbit comparison of maximum out-of-plane distance and required distance to avoid eclipses.

[4] NASA Jet Propulsion Laboratory. Three-body periodic orbits, 2020.

[5] Kathryn Davis, George Born, and Eric Butcher. Transfers to earth–moon l3 halo orbits. *Acta Astronautica*, 88:116–128, 2013.

[6] Peter Musen. The influence of the solar radiation pressure on the motion of an artificial satellite. *Journal of Geophysical Research*, 65(5):1391–1396, 1960.

[7] C Frueh, K Howell, K DeMars, S Bhadauria, and M Gupta. Cislunar space traffic management: Surveillance through earth-moon resonance orbits. In *8th European Conference on Space Debris*, 2021.

[8] Thomas Pavlak and Kathleen Howell. Strategy for optimal, long-term stationkeeping of libration point orbits in the earth-moon system. In *AIAA/AAS Astrodynamics Specialist Conference*, page 4665, 2012.

[9] Carolin Frueh, Kathleen Howell, Kyle J DeMars, and Surabhi Bhadauria. Cislunar space situational awareness. In *31st AIAA/AAS Space Flight Mechanics Meeting*, 2021.

[10] Fred Espenak. Eclipses and the moon's orbit, 2012.

[11] Luc Maisonobe, Véronique Pommier, and Pascal Parraud. Orekit: An open source library for operational flight dynamics applications. In *4th International Conference on Astrodynamics Tools and Techniques*, pages 3–6, 2010.

[12] CC Chow, CJ Wetterer, K Hill, C Gilbert, D Buehler, and J Frith. Cislunar periodic orbit families and expected observational features. In *Proceedings of the Advanced Maui Optical and Space Surveillance (AMOS) Technologies Conference, page*, 2020.